JOURNAL OF GEOPHYSICAL RESEARCH, VOL. 101, NO. C5, PAGES 12,071–12,078, MAY 15, 1996

Effects of wave breaking on the surface drift

Arne Melsom
Norwegian Meteorological Institute, Oslo, Norway

Abstract. The present paper is an investigation of the motion induced in the ocean by breaking waves. The theory that is presented here addresses two related problems concerning such motion. First, several parameterizations for transfer of momentum during breaking are examined. Second, attempts are made to describe the surface drift and the vertical structure of motion that results from multiple breaking events. It is shown that the various parameterizations of breaking events are robust in the sense that they qualitatively and quantitatively give similar results. However, for description of the vertical structure of the current, the Reynolds stresses must be parameterized. For this purpose, we will here adopt the concept of eddy viscosity. It is demonstrated that wave breaking enhances motion close to the surface and retards motion in the deeper parts of the ocean. Also, the drift induced by multiple events of breaking is significant, and it is only slightly deflected from the direction of wave propagation.

1. Introduction

The circulation of the ocean's surface layer has traditionally received much attention. This is due to a variety of problems ranging from spill simulations to interpretation of satellite data where an accurate description of the near-surface circulation is required. An important feature of this circulation is the motion associated with gravity waves. Most of the analytical theory in this field has been developed for constant amplitude waves and frictionally damped waves [*Lamb*, 1932; *Longuet-Higgins*, 1953]. However, under the action of the wind, the wave amplitude will generally increase in time (or space). The main purposes of the present paper are to develop a robust model for a breaking event and to investigate the effect of multiple events of time dependent wave breaking on the surface drift of the ocean.

The total mean atmospheric stress does not only induce ocean currents through the action of the shear stress alone [*Ekman*, 1905] but also supplies momentum to growing surface waves. If we disregard the effect of friction and average over one inertial cycle, no net Lagrangian motion is induced by constant amplitude waves in a rotating ocean [*Ursell*, 1950; *Hasselmann*, 1970]. When viscosity is taken into account so that the waves are allowed to decay, average Lagrangian motion is present, but the volume flux remains zero [*Weber*, 1983; *Weber and Førland*, 1990].

After the wind has been acting on the ocean surface for some time, the amplitude of the fastest growing wave component will reach a critical steepness at which the wave breaks. Thus the amplitude is reduced within a comparatively short time interval. At subsequent times, the waves will rebuild due to the additional momentum that is provided by the continued action of the wind. In this way, an average balance between energy input from the wind and dissipation due to repeated events of wave breaking will evolve as the sea becomes fully developed.

In a recent paper, *Weber and Melsom* [1993a] examined the nonlinear drift current that develops due to wind and waves. Several cases covering damped waves as well as growing waves were investigated. It was demonstrated that the drift that is associated with growing waves does not exhibit inertial oscillations before breaking occurs. Furthermore, it was shown that the wave-induced surface current is almost a linear function of the friction velocity. However, the Lagrangian formulation that was applied in that paper cannot handle wave breaking due to the discontinuities of material surfaces that are associated with such breaking.

Following that paper, *Weber and Melsom* [1993b] considered the volume flux in a saturated sea. They concluded that mean Lagrangian momentum transfer from the atmosphere to the ocean via surface waves occurs only in the presence of growing waves. Hence one role of breaking is that it provides the necessary basis for lasting wave growth and a corresponding momentum transfer. However, only vertically integrated properties were considered in the latter paper. The present paper is an attempt to take the theory a step further by examining the vertical distribution of the induced current. A crucial problem involved in such a theory will be to describe the transfer of momentum from the waves to the mean drift during events of wave breaking. Hence an entire section in the present paper is devoted to this problem.

Paper number 96JC00584.
0148-0227/96/96JC-00584$09.00

2. Mathematical Formulation

The method of separation of wave motion, mean motion, and high-frequency motion that will be applied here is the same as that of *Weber and Melsom* [1993b]. On the basis of an assumption of distinct timescales, the Eulerian pressure and velocity fields are divided into three separate parts:

$$(p,\mathbf{v}) = (p',\mathbf{v}') + (\hat{p},\hat{\mathbf{v}}) + (\bar{p},\bar{\mathbf{v}}) \tag{1}$$

Here primes, carets, and overbars denote small-scale turbulent fluctuations, wave motion, and mean motion, respectively. By application of time-averaging processes, equations for the wave motion and for the mean motion may be developed. The two time-averaging processes that are employed are denoted by < > and { }. They correspond to temporal integration over periods that remove linear turbulent and linear wave quantities, respectively.

We restrict ourselves to considering motion confined to the ocean's mixed layer and take the density ρ to be constant. Furthermore, we assume that the ocean depth is infinite in mathematical terms. A Cartesian frame of reference is applied, with the vertical z axis being positive upward. The undisturbed horizontal surface is taken to define $z = 0$. We will consider motion in an ocean that rotates about the vertical axis with a constant angular velocity $f/2$. The governing Eulerian equations for wave motion and mean motion become

$$\begin{aligned}\frac{\partial\hat{\mathbf{v}}}{\partial t} + \hat{\mathbf{v}}\cdot\nabla\hat{\mathbf{v}} - \{\hat{\mathbf{v}}\cdot\nabla\hat{\mathbf{v}}\} + f\mathbf{k}\times\hat{\mathbf{v}} &= -\nabla\frac{\hat{p}}{\rho} \\ &+ \nu_m\nabla^2\hat{\mathbf{v}} + \nabla\cdot\left[-\hat{\mathbf{v}}\bar{\mathbf{v}} - \bar{\mathbf{v}}\hat{\mathbf{v}} - <\mathbf{v}'\mathbf{v}'> + \{<\mathbf{v}'\mathbf{v}'>\}\right]\end{aligned} \tag{2}$$

and

$$\begin{aligned}\frac{\partial\bar{\mathbf{v}}}{\partial t} + \bar{\mathbf{v}}\cdot\nabla\bar{\mathbf{v}} + f\mathbf{k}\times\bar{\mathbf{v}} &= \\ -\nabla\frac{\bar{p}}{\rho} - g\mathbf{k} + \nu_m\nabla^2\bar{\mathbf{v}} &+ \nabla\cdot\left[-\{<\mathbf{v}'\mathbf{v}'>\} - \{\hat{\mathbf{v}}\hat{\mathbf{v}}\}\right]\end{aligned} \tag{3}$$

respectively. Here g is the vertical acceleration due to gravity, ν_m is the molecular viscosity coefficient, and ∇ denotes the gradient operator. For details on the derivation of these equations the reader is referred to *Weber and Melsom* [1993b]. As in that paper, we will consider motion associated with a monochromatic surface wave that travels in the x direction,

$$\zeta = \zeta_0 e^{\beta t}\cos(kx - \omega t) \tag{4}$$

where k is the wave number, ω is the frequency, and β is the growth rate. The corresponding wave velocities are then the solutions of (2) with appropriate boundary conditions. The nonlinear terms involving $\hat{\mathbf{v}}$ and $\bar{\mathbf{v}}$ are neglected. This will restrict the accuracy of the description of the wave field close to breaking. However, the amount of momentum transfer from wave motion to mean motion should not be affected significantly by this simplification. Thus, in the few seconds around breaking when the nonlinear terms cannot be neglected, a bulk parameterization is used by taking advantage of the principle of momentum conservation.

In a study of monochromatic waves we assume that $\nabla\cdot<\mathbf{v}'\mathbf{v}'> \sim \mathbf{A}\cos\omega t + \mathbf{B}$ for the separation (1) to be meaningful. Furthermore, it is assumed that there is a relatively small contribution from $<\mathbf{v}'\mathbf{v}'>$ at frequencies close to ω, i.e., $|\mathbf{A}| << |\mathbf{B}|$. Then, the two terms in (2) that involve the turbulent Reynolds stress will tend to cancel each other, since $\nabla\cdot[-<\mathbf{v}'\mathbf{v}'> + \{<\mathbf{v}'\mathbf{v}'>\}] \sim -\mathbf{A}\cos\omega t$. Hence their combined effect on the wave motion will be neglected in (2). Due to their small magnitude, viscous stresses will also be disregarded.

To lowest order in f/ω, the motion that corresponds to the monochromatic wave (4) now becomes

$$\begin{aligned}\hat{u} &= \zeta_0\omega e^{\beta t + kz}\left[\cos(kx-\omega t) - \frac{\beta}{\omega}\sin(kx-\omega t)\right] \\ \hat{v} &= \zeta_0 f e^{\beta t + kz}\sin(kx-\omega t) \\ \hat{w} &= \zeta_0\omega e^{\beta t + kz}\left[\sin(kx-\omega t) + \frac{\beta}{\omega}\cos(kx-\omega t)\right]\end{aligned} \tag{5}$$

In the presence of wave motion, the velocities of the individual particles (the Lagrangian velocities) become different from the corresponding Eulerian velocities. Transformation of the Eulerian problem to Lagrangian description may be carried out utilizing the formula

$$\mathbf{v}_L = \mathbf{v} + \mathbf{v}_S = \mathbf{v} + \left(\int_{t_0}^{t}\mathbf{v}_L(\mathbf{r}_0,\tau)\,d\tau\right)\cdot\nabla_0\mathbf{v}_L(\mathbf{r}_0,t) \tag{6}$$

[*Phillips*, 1977]. Here the subscript L denotes the Lagrangian, $\mathbf{v}$ is the Eulerian velocity vector, and $\mathbf{v}_S$ is the Stokes drift. An approximate solution for the mean Stokes drift is given by

$$\bar{\mathbf{v}}_S = \overline{\left(\int_{t_0}^{t}\hat{\mathbf{v}}\,d\tau\right)\cdot\nabla\hat{\mathbf{v}}} = \zeta_0^2\omega k\, e^{2(kz+\beta t)}\,\mathbf{i} \tag{7}$$

from (5), correct to second order in wave amplitude. Keeping in mind that the wave amplitude is $\zeta_0 e^{\beta t}$, this is the well-known result of *Stokes* [1847].

We will also disregard effects of the molecular viscosity for the mean motion. Furthermore, the wave stress tensor $\{\hat{\mathbf{v}}\hat{\mathbf{v}}\}$ follows from (5), and the equation for the horizontal mean Lagrangian motion becomes

$$\frac{\partial\bar{\mathbf{v}}_L}{\partial t} + f\mathbf{k}\times\bar{\mathbf{v}}_L - \frac{\partial}{\partial z}\nu\frac{\partial\bar{\mathbf{v}}_L}{\partial z} = \frac{\partial\bar{\mathbf{v}}_S}{\partial t} - \frac{\partial}{\partial z}\nu\frac{\partial\bar{\mathbf{v}}_S}{\partial z} \tag{8}$$

where an eddy viscosity formulation has been applied for the mean turbulent Reynolds stresses. The terms on the left-hand side of (8) represent acceleration, effects of rotation, and turbulent momentum diffusion, respectively. The first term on the right-hand side arises from the fact that the periodic motion possesses a time dependent Lagrangian mean drift. The final term in (8) appears as a result of the transformation of the momentum diffusion term. Observe that it is necessary to retain the Coriolis term in the wave motion (5) to obtain (8) [*Hasselmann*, 1970].

In order to solve this problem, the appropriate boundary conditions must be imposed. For large depths the current induced by wind and waves must vanish, i.e.,

$$\bar{\mathbf{v}}_L \to 0, \quad z \to -\infty \tag{9}$$

The surface boundary condition is obtained by requiring a continuous stress. Then,

$$\overline{\mathbf{T}_0} = \rho\nu\frac{\partial\bar{\mathbf{v}}}{\partial z}(z=0) = \rho\nu\frac{\partial}{\partial z}\left(\bar{\mathbf{v}}_L - \bar{\mathbf{v}}_S\right)(z=0) \tag{10}$$

where $\overline{\mathbf{T}_0}$ is the mean tangential stress that acts on the surface. Since the initial wave amplitude is ζ_0, the ocean has been exposed to a wind stress for some time prior to $t = 0$. Hence there is no obvious choice of initial condition for the mean motion. We shall take

$$\bar{\mathbf{v}}_L\,(t=0) = \bar{\mathbf{v}}_S\,(t=0) \tag{11}$$

which is consistent with the wave motion present at that time.

Obviously, the partial differential equations for momentum and mass are not valid during breaking events. Thus it is convenient to divide the problem by considering the drift induced by wave breaking separate from the drift that is associated with growing waves. As we shall see in the next section, it is then possible to calculate the drift induced by breaking events by applying the principle of momentum conservation.

3. Effects of an Event of Wave Breaking

First, we examine effects of one isolated breaking event. Due to the short timescale of a breaking event and the rapid development of an associated drift current, we can safely disregard effects of rotation in the present context. The breaking process itself is a very complicated phenomenon which we will not attempt to describe here. Instead, we take advantage of the principle of momentum conservation of an isolated system. Take $\Delta\mathbf{M}_E$ to be the amount of Eulerian momentum that is lost from the wave motion when the amplitude is reduced by $\Delta\zeta$. Then,

$$\overline{\Delta\mathbf{M}_E} = \rho\Delta\zeta\;\zeta_0\omega\mathbf{i} = \overline{\Delta\mathbf{M}_1} + \overline{\Delta\mathbf{M}_2\,(z<\zeta)} \tag{12}$$

where $\Delta\mathbf{M}_1$ and $\Delta\mathbf{M}_2$ are given below.

One consequence of breaking is that momentum is lost from the periodic wave motion at the surface due to amplitude reduction. This process, where mass moving in the wave propagation direction (dark shading) is replaced by mass moving in the opposite direction (light shading) after breaking, is described in Figure 1a. We find

$$\Delta\mathbf{M}_1 = \rho\int_{\zeta_0\cos\varphi}^{(\zeta_0+\Delta\zeta)\cos\varphi}\hat{\mathbf{v}}\,dz \quad\Rightarrow\quad \overline{\Delta\mathbf{M}_1} = \frac{1}{2}\overline{\Delta\mathbf{M}_E} \tag{13}$$

where φ is the phase function.

Moreover, the wave motion will be affected instantaneously in the entire water column through the change in the pressure gradient that is associated with the drop in amplitude. For the momentum transfer below the material interface $\eta = z + \zeta_0\,e^{2kz}\cos\varphi$ we find

$$\Delta\mathbf{M}_2\,(z<\eta) = \rho\int_{-\infty}^{\eta}\Delta\hat{\mathbf{v}}\,dz$$

$$\Rightarrow\quad \overline{\Delta\mathbf{M}_2\,(z<\eta)} = \frac{e^{2kz}}{2}\overline{\Delta\mathbf{M}_E} \tag{14}$$

The momentum that is transferred to the mean motion by this process is depicted in Figure 1b (shaded area).

Finally, wave breaking results in a change in the Stokes drift. Note that

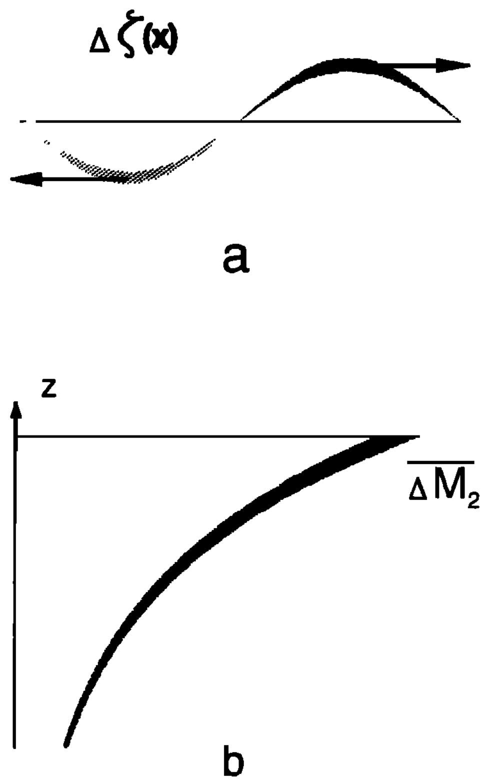

Figure 1. Momentum conversion from periodic motion to mean motion during breaking. (a) Sketch of conversion due to shifted distribution of mass. The wave propagates to the right. (b) Sketch of mean momentum lost from the periodic motion $\hat{\mathbf{v}}$ due to reduced velocities after breaking. The magnitude of the amplitude reduction has been exaggerated. See the text for details.

$$\rho\int_{-\infty}^{0}\overline{\Delta\mathbf{v}_S}\,dz = -\,\overline{\Delta\mathbf{M}_E} \tag{15}$$

so the vertically integrated Lagrangian momentum is not affected by wave breaking [*Weber and Melsom*, 1993b].

In the case of decaying waves, the transfer of wave momentum to the mean drift may be parametrized by a virtual wave stress $\mathbf{T}_{vw}$ that acts on the mean current at the surface [*Longuet-Higgins*, 1969]. In the present context, the momentum that is lost at the surface due to amplitude reduction will be redistributed by turbulent stresses, completely analogous to Longuet-Higgins' case. As was pointed out above, momentum is lost from the periodic motion throughout the entire water column. In order to conserve the overall momentum, we also introduce an initial drift $\bar{\mathbf{v}}_0$, so that

$$\overline{\Delta\mathbf{M}_E} = \overline{\Delta\mathbf{M}_1} + \overline{\Delta\mathbf{M}_2} = \int_0^{\infty}\overline{\mathbf{T}_{vw}}\,dt + \rho\int_{-\infty}^{0}\bar{\mathbf{v}}_0\,dz \tag{16}$$

The forcing terms in (8) are associated with the drift current that is induced by growing waves and the wind stress. We will return to this problem in a later section. The momentum equation for the mean Lagrangian drift induced by wave breaking, $\bar{\mathbf{v}}_B$, then becomes

$$\frac{\partial \bar{\mathbf{v}}_B}{\partial t} - \frac{\partial}{\partial z}\nu\frac{\partial \bar{\mathbf{v}}_B}{\partial z} = \mathbf{0} \tag{17}$$

The initial condition is

$$\begin{aligned} \bar{\mathbf{v}}_B(t=0) &= \bar{\mathbf{v}}_0 + \overline{\Delta \mathbf{v}}_S \\ \overline{\Delta \mathbf{v}}_S &= -2\Delta\zeta\,\zeta_0\omega k\, e^{2kz}\,\mathbf{i} \end{aligned} \tag{18}$$

and the boundary condition at the surface becomes

$$\overline{\mathbf{T}}_{vw} = \rho\nu\frac{\partial \bar{\mathbf{v}}_B}{\partial z}(z=0) \tag{19}$$

Qualitatively, (17) - (19) are a problem involving mixing of momentum from the surface to the ocean's interior. Hence a good parameterization of the Reynolds stress is necessary for obtaining the correct development of the vertical distribution of momentum. Here our aim is to test various ways of parameterizing the transfer of momentum due to a breaking event. For such intercomparisons the simple assumption of a constant eddy viscosity coefficient will suffice. It may be argued that in a saturated sea the strong turbulent mixing of the wave zone will lead to quasi-homogeneous conditions in this region. This argument supports the use of a constant value for ν.

3.1. Virtual Wave Stress as an Impulse

Assume that the momentum is instantaneously transferred to the mean flow when a breaking event occurs. We may then take

$$\begin{aligned} \overline{\mathbf{T}}_{vw} &= \frac{1}{2}\rho\Delta\zeta\,\zeta_0\omega\,\delta(t)\,\mathbf{i} \\ \bar{\mathbf{v}}_0 &= \frac{1}{\rho}\frac{d}{dz}\overline{\Delta\mathbf{M}}_2(z<\eta) = -\frac{1}{2}\overline{\Delta\mathbf{v}}_S \end{aligned} \tag{20}$$

where δ is the Dirac delta function. The solution of (17) with conditions given by (20) is obtained by Laplace transformation and subsequent inverse transformation, yielding

$$u_1 = \Delta\zeta\,\zeta_0'\omega\left[\frac{1}{2}\frac{e^{-z^2/(4\nu t)}}{\sqrt{\pi\nu t}} - \frac{4}{\pi}k^2\int_0^\infty \frac{\cos(xz)\,e^{-\nu t x^2}}{x^2+4k^2}dx\right] \tag{21}$$

Note that this expression is not well defined for $t = 0$ due to the impulse imposed at the surface at this time. However, we have

$$\lim_{t\to 0} u_1(z<0) = \frac{1}{2}\Delta u_S \tag{22}$$

in concord with the initial condition.

The temporal development and vertical profiles of u_1 are depicted in Figure 2a and 2b, respectively. We have chosen $k = 0.2$ m^{-1} and $\nu = 1 \times 10^{-3}$ m^2 s^{-1}. The numbers on the vertical axis in Figure 2a and the horizontal axis in Figure 2b represent the nondimensional drift u_r, defined by

$$u_r = \frac{u_1}{\Delta\zeta\,\zeta_0\omega k} \tag{23}$$

The horizontal axis in Figure 2a corresponds to nondimensional time $t_r = \omega t/2\pi$, the number of wave periods after the breaking event. The vertical axis in Figure 2a denotes the nondimensional depth $z_r = kz$. The curves 1, 2, and 3 in Figure 2a depict the evolution of the drift velocities at depths $z_r = 0$, -0.05, and -0.2, respectively. In Figure 2b, curves 1, 2, and 3 display the velocity profiles for times $t_r = 5$, 20, and 100, respectively.

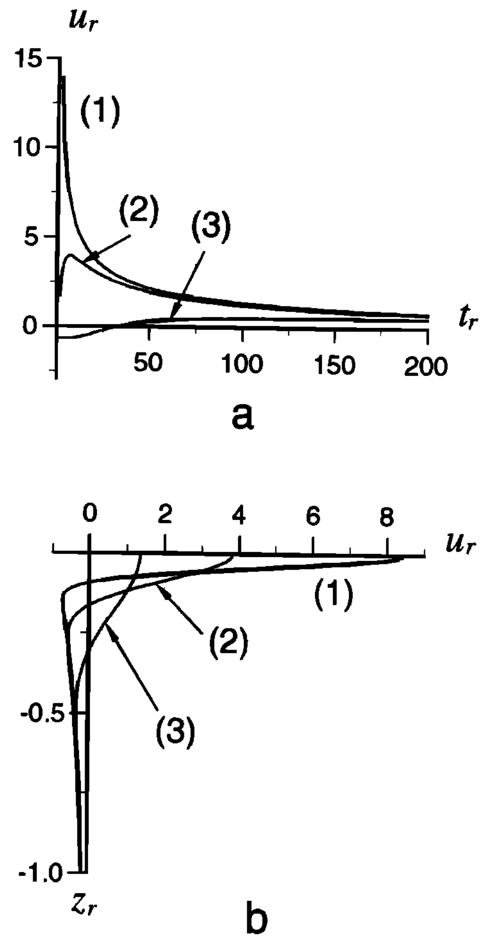

Figure 2. Nondimensional drift velocity induced by an event of wave breaking. Momentum conversion was parameterized according to (20). (a) Induced drift as a function of nondimensional time t_r after the breaking event. Curves 1, 2, and 3 correspond to nondimensional depths $z_r = 0$, -0.05 and -0.2, respectively. (b) Induced drift as a function of nondimensional depth z_r. Curves 1, 2, and 3 show the velocity profiles at nondimensional times $t_r = 5$, 20, and 100, respectively. We have taken $k = 0.2$ m^{-1} and $\nu = 1 \times 10^{-3}$ m^{2}s^{-1}. See the text for further details.

3.2. Time Dependent Virtual Wave Stress

Although wave breaking is a phenomenon with a very short duration, it does probably not behave as a delta function. In order to assess the sensibility of the solution (21) to the temporal development of breaking, we take

$$\begin{aligned} \overline{\mathbf{T}}_{vw} &= \frac{1}{2}\rho\Delta\zeta\,\zeta_0\omega\kappa\, e^{-\kappa t}\,\mathbf{i} \\ \bar{\mathbf{v}}_0 &= -\frac{1}{2}\overline{\Delta\mathbf{v}}_S \end{aligned} \tag{24}$$

Here, κ^{-1} is a timescale that corresponds to exponential decay in the intensity of the breaking event. The solution is again obtained by Laplace transforms and can be written as

$$u_2 = \Delta\zeta\ \zeta_0 \omega k \times \left[\frac{1}{2k}\sqrt{\kappa/\nu}\ \sin\left(z\sqrt{\kappa/\nu}\right) e^{-\kappa t} - \frac{1}{\pi}\int_0^\infty \left(\frac{4k}{x^2+4k^2} + \frac{1}{k}\frac{1}{\nu}\frac{\kappa}{x^2-\kappa/\nu} \right) \cos(xz)\, e^{-\nu t x^2} dx \right] \quad (25)$$

At first sight this expression may seem somewhat odd. The first term in the brackets does not go away even at an infinite depth, and one of the terms in the integrand has a singularity at $x = (\kappa/\nu)^{1/2}$. However, at large depths the contribution from the singularity will cancel the term outside of the integral. It may, for example, be shown that u_2 satisfies the initial condition.

Take $\kappa = \omega/2\pi$, that is, the exponential decay rate of the forcing is equal to the wave period. In Figure 3, curve 1 then displays the nondimensional depth at which the difference between the solutions u_2 and u_1 is 5% of u_1, as a function of nondimensional time. The domain above the curve corresponds to larger differences; below the curve, the differences are less than 5% of u_1. We observe that when $t_r > 3$, the differences between the two solutions are smaller than 5% at all depths.

3.3. Initial Distribution of Momentum

It may be argued that the process of wave breaking has a certain vertical extent and is not really acting at the very surface only. In order to examine the effect of an initial vertical distribution of the transformed momentum $\overline{\Delta \mathbf{M}}_1$, take

$$\overline{\mathbf{T}}_{vw} = \mathbf{0}$$
$$\bar{\mathbf{v}}_0 = \frac{1}{2}\left(\Delta\zeta\ \zeta_0\omega\alpha\, e^{\alpha z} - \overline{\Delta u_S}\right)\mathbf{i} \quad (26)$$

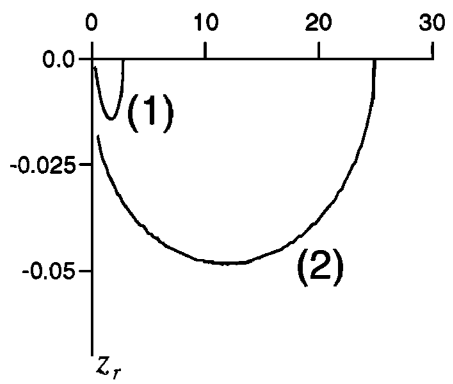

Figure 3. Nondimensional depth z_r at which the velocity difference arising from two different parameterizations of breaking is 5%, as a function of nondimensional time t_r. Curves (1) and (2) correspond to 5% velocity differences in (21) and (25), and (21) and (27), respectively. The domain to the right and below the curves shows the depths where this difference is less than 5% at the corresponding times.

Thus α is the rate of vertical decay of the initial distribution of $\overline{\Delta \mathbf{M}}_1$. As previously, Laplace transforms allow us to determine the solution, which in this case becomes

$$u_3 = \frac{1}{\pi}\Delta\zeta\ \zeta_0\omega k \times \int_0^\infty \left[\frac{\alpha^2}{x^2+\alpha^2} - \frac{4k^2}{x^2+4k^2} \right] \cos(xz)\ e^{-\nu t x^2} \quad (27)$$

The case of momentum transfer by a virtual wave stress impulse can be reproduced from this solution by taking the limit $\alpha \to \infty$, i.e.,

$$u_1 = \lim_{\alpha \to \infty} u_3 \quad (28)$$

An infinitely large value of α corresponds to introducing a finite amount of momentum in an infinitely thin surface layer at $t = 0$. This is exactly the effect of an initial virtual wave stress impulse. The vertical scale α^{-1} of the initial distribution of $\overline{\Delta \mathbf{M}}_1$ must be related to the vertical scale of wave breaking, which is the generating mechanism. Hence we expect α^{-1} to be proportional to $\Delta\zeta$. For $k = 0.2\ \mathrm{m}^{-1}$, we have $\Delta\zeta \sim 0.015 - 0.15$ m, depending on the amount of energy being transferred [*Weber and Melsom*, 1993b]. In Figure 3, curve 2 depicts the nondimensional depth at which the difference between the solutions u_3 and u_1 is 5% of u_1, as a function of nondimensional time. Here we have used $\alpha = 10\ \mathrm{m}^{-1}$. We observe that when $t_r > 27$, the difference between the two solutions is smaller than 5% at all depths.

4. Multiple Breaking Events and Drift Currents

The problem that remains to be solved is given by (8) - (11) where $\mathbf{v}_S$ is the Stokes drift associated with waves with growing amplitude. Denoting the drift induced by wind and growing waves by $\bar{\mathbf{v}}_\beta$ and that induced by N breaking events by $\bar{\mathbf{v}}_{NB}$, we have

$$\bar{\mathbf{v}}_L = \bar{\mathbf{v}}_{NB} + \bar{\mathbf{v}}_\beta \quad (29)$$

We may introduce a complex drift

$$w = \bar{u}_L + i\bar{v}_L \quad (30)$$

Here, i is the complex unit number. The various parameterizations that were explored in the previous section differed significantly only the first minute or so after the breaking of the wave. Thus, when examining effects of multiple breaking events, only one parameterization will be considered. In this section, momentum transfer due to wave breaking will be assumed to act as a virtual wave stress that behaves like a δ function in time, i.e., (20).

It will be demonstrated that the drift that is induced by multiple breaking events develops on a timescale of several hours. When the Coriolis force is taken into account, it can easily be shown that the induced drift becomes

$$w_B(t,z) = e^{-ift} u_1(t,z) \quad (31)$$

where u_1 is given by (21). This relation follows from the substitution property of Laplace transforms and is due to the simplicity of the transformed Dirac delta function

$\{ L[\delta(t)] = 1 \}$. Thus it only holds for u_1. Assuming a constant interval ΔT_B between two subsequent breaking events, the drift w_{NB} induced by N breaking events becomes

$$w_{NB} = \sum_{n=1}^{N} w_B [t - (n-1)\Delta T_B, z] \tag{32}$$

when breaking occurs at the critical amplitude

$$\zeta_c = \zeta_0 e^{\beta \Delta T_B} \tag{33}$$

The solution for w_β in the simple case of a constant eddy viscosity is determined:

$$w_\beta = \frac{T_0}{2\rho\nu}\left[(1-i) E e^{(1+i)z/E} - \frac{4}{\pi} e^{-ift} \int_0^\infty \frac{\cos(xz)\, e^{-\nu t x^2}}{x^2 + (1+i)E^{-2}} dx \right]$$

$$+ \zeta_0^2 \omega k \times$$

$$\left[(1-a) e^{2kz} + (1-i) akE\, e^{(1+i)z/E} - \right.$$

$$\left. \frac{4ak}{\pi} \int_0^\infty \left(\frac{1}{x^2 + (1+i)E^{-2}} - \frac{1}{x^2 + 4k^2} \right) \cos(xz)\, e^{-\nu t x^2} dx \right] \tag{34}$$

$E = \sqrt{2\nu/f}$ is the Ekman depth, and a is a nondimensional coefficient given by

$$a = \frac{(2\beta/f - i)(2k^2E^2 + i)}{4k^4E^4 + 1} \tag{35}$$

The steady volume flux becomes

$$W = \lim_{t\to\infty} \int_{-\infty}^{0} w\, dz = -\frac{i}{f}\left[\frac{T_0}{\rho} + \zeta_0^2 \omega\beta \right] \tag{36}$$

In the saturation range, the volume flux induced by the turbulent wind stress at the surface, W_{wind}, and the flux induced by growing waves, W_{wave}, are of comparable magnitude [*Mitsuyasu*, 1985; *Weber and Melsom*, 1993b]. Here (36) yields

$$\frac{W_{\text{wind}}}{W_{\text{wave}}} = \frac{T_0}{\rho \zeta_0^2 \omega\beta} \tag{37}$$

It has been demonstrated both analytically [*Jacobs*, 1987; *Weber and Melsom*, 1993a] and experimentally [*Plant*, 1982; *Mitsuyasu and Honda*, 1982] that the nondimensional quantities β/ω and U_*/C are related in accordance with

$$\frac{\beta}{\omega} = K\left(\frac{U_*}{C}\right)^2 \tag{38}$$

for the most rapidly growing wave. Here U_* is the friction velocity in the logarithmic bottom layer of the atmosphere, and $C = \omega/\kappa$ is the wave phase speed. Introducing the wave steepness parameter $\Lambda = \zeta_0 k$, we find

$$\frac{W_{\text{wind}}}{W_{\text{wave}}} = \frac{T_0}{\rho_a U_*^2} \frac{\rho_a/\rho}{\Lambda^2 K} = \frac{\tau s}{\Lambda^2 K} \tag{39}$$

In (39), τ is the ratio of the wind stress at the ocean surface (T_0) to the total stress in the logarithmic layer of the atmosphere ($\rho_a U_*^2$), and $s = \rho_a/\rho$, ρ_a being the density of the air. In the quasi-steady conditions of a saturated sea, momentum cannot accumulate in the logarithmic bottom layer of the atmosphere. Hence we must also have

$$\frac{W_{\text{wind}}}{W_{\text{wave}}} = \frac{\tau}{1-\tau} \tag{40}$$

We take $s = 1.2 \times 10^{-3}$ and $\Lambda = 0.3$ for a fully developed sea. From his survey of field and laboratory observations, *Plant* [1982] finds that the coefficient K lies in the range 1×10^{-2} to 3×10^{-2}. Investigating two continuous wave spectra due to *Phillips* [1958] and *Toba* [1973], *Weber and Melsom* [1993b] found $\tau \sim 0.4$. However, $\tau = 0.4$ gives values for K that are outside the stated range. Thus we shall take $K = 1 \times 10^{-2}$ and $\tau = 0.25$, which satisfy (39) and (40) simultaneously. Denote the relative energy that is lost from the wave motion due to a single breaking by Δe, i.e.,

$$\Delta e = \frac{\zeta_c^2 - \zeta_0^2}{\zeta_0^2} = e^{2\beta\Delta T_B} - 1 \tag{41}$$

We take $\nu = 10^{-3}$ m^2 s^{-1}, $U_*/C = 10^{-1}$ [*Jacobs*, 1987], and $f = 1.2 \times 10^{-4}$ s^{-1}. When $k = 0.2$ m^{-1}, we find $\beta = 1.4 \times 10^{-4}$ s^{-1} from (38). Experimental results indicate that Δe lies between 10^{-2} and 10^{-1} [*Melville and Rapp*, 1985]. We choose $\Delta e = 5 \times 10^{-2}$, then the interval ΔT_B becomes 170 s. In Figure 4, the surface drift induced by multiple breaking events, $\bar{\mathbf{v}}_{NB}$, is depicted as hodograph 1, whereas the corresponding drift due to wind and growing waves, $\bar{\mathbf{v}}_\beta$, is displayed by hodograph 2. The numbers on the axes represent nondimensional drift velocities. Since $\bar{\mathbf{v}}_\beta$ is independent of ζ_c^2-ζ_0^2, it is not practical to make the velocity components nondimensional using (23). Instead, the drift velocities have been divided by the initial surface Stokes drift $u_{S;0} = \zeta_0^2\omega k$. The asterisks represent the surface drift vector after the cor-

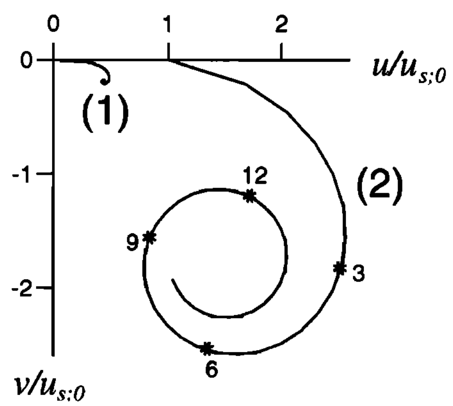

Figure 4. Hodographs of the nondimensional surface drift. Hodograph 1 displays the part of the surface drift that is induced by wave breaking when the wave energy Δe is reduced by 5% in each event of breaking. Hodograph 2 displays the part of the surface drift that is induced by wind and growing waves. The numbered asterisks on hodograph 2 denote evolution time in pendulum hours. See the text for details.

responding number of pendulum hours. The temporal development of hodograph 1 is similar to that of hodograph 2.

We define r as the ratio of the surface drift induced by wave breaking to the drift induced by wind and growing waves, i.e.,

$$r = \lim_{t \to \infty} \left| \bar{\mathbf{v}}_{NB} / \bar{\mathbf{v}}_{\beta} \right| (z = 0) \tag{42}$$

From Figure 4, we find that r is around 20%. The sensitivity of the value for this ratio to various parameters will be discussed in the final section.

5. Discussion and Concluding Remarks

In many ways, the descriptions of waves and wave breaking that have been adopted here are rather idealized. To begin with, only a single Fourier component is considered. Breaking of this monochromatic wave constitutes a somewhat peculiar process in the present formulation, insofar as the breaking events occur simultaneously everywhere at regular time intervals. Consequently, the results that have been obtained in this paper should be interpreted as representing the statistical properties of the state of a saturated sea.

Let us first consider the drift that is induced by momentum transfer in the case of an isolated event of wave breaking. The principle of momentum conservation yields the initial drift and forcing due to breaking. After breaking, diffusion causes a redistribution of momentum in the vertical. Since the forcing in principle is confined to the surface, the local maximum of the drift will be reached earlier at small depths than at large depths. For the same reason, the maximum drift velocity at any given time is the value at the surface. These features of momentum diffusion can all be observed in Figures 2a and 2b.

Furthermore, it is revealed from Figure 3 that parameterization of momentum transfer due to wave breaking is a robust procedure, in the sense that the various descriptions (20), (24), and (26) yield only minor differences. To the author's knowledge, this is a new result which will hopefully prove to be beneficial for future investigations of problems that involve wave breaking. The success of the parameterization by a delta function is due to the scales involved. Both the vertical extent and the temporal development of the induced drift are of much larger scales than those associated with the process of wave breaking.

From (21) we observe that the temporal decay of the surface drift induced by a breaking event is proportional to $t^{-1/2}$ for large times. Since this is a rather small rate of decay, we anticipate that the combined effect of multiple breaking events significantly enhances the surface drift. In fact, computations reveal that the quasi-steady surface drift induced by multiple breaking events is typically 5 times the magnitude of the surface drift that is induced by the most recent of these events.

In his classic paper, *Ekman* [1905] calculated the wind-induced current assuming a constant eddy viscosity. Then, the surface drift is deflected 45° to the right of the wind stress vector (in the northern hemisphere). On the other hand, observations indicate that the deflection angle is much smaller than this value. On the basis of an eddy viscosity that increases linearly with depth, *Madsen* [1977] demonstrated that the wind-induced surface drift becomes more parallel with the wind. However, it should be pointed out that this linear profile was originally developed for flow in the vicinity of solid boundaries such as the bottom or an ice cover [*Melsom*, 1993] and not for a free interface. In relation to this discussion, we observe from Figure 4 that the presence of wave breaking decreases the deflection of the surface drift from the direction of the wind stress.

Weber and Melsom [1993b] showed that there is no integrated volume flux induced by wave breaking. Accordingly, the influence of wave breaking on the surface drift will to a large degree be determined by the level of turbulent mixing of momentum. A high level of turbulent mixing leads to small vertical gradients. Then, since the flux is zero, the effect of wave breaking on the surface drift becomes relatively small. This effect is clearly shown in Figure 5a. There, the ratio of the steady wave-induced drift to the drift induced by wind and growing waves, r, is depicted as a function of the eddy viscosity ν. The values for ν are given in SI units on the horizontal logarithmic axis. Curve 1 has been calculated based on the same parameter values as in Figure 4 (except for ν).

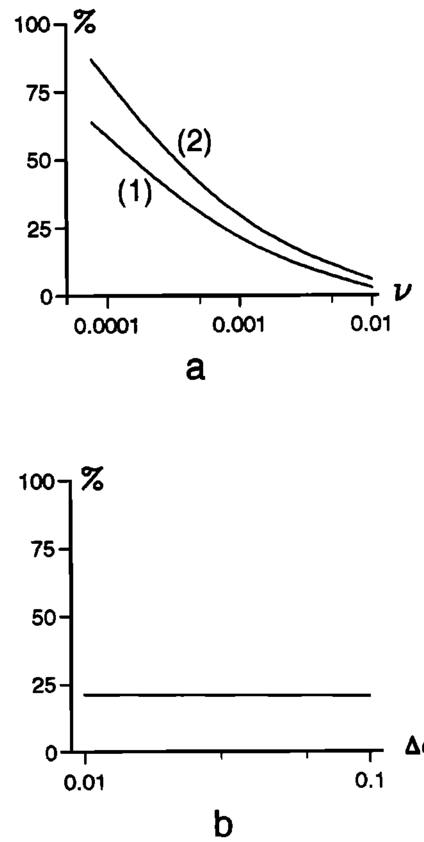

Figure 5. The ratio of the steady surface current induced by wave breaking $\bar{\mathbf{v}}_{NB}$ to the remaining drift $\bar{\mathbf{v}}_{\beta}$, r. (a) Here r is depicted as a function of eddy viscosity ν (in square meters per second). Curve 1 corresponds to the parameter values chosen for Figure 4, whereas curve 2 displays the ratio when $K = 2.7 \times 10^{-2}$ and $\tau = 0.4$. (b) Here r is depicted as a function of the relative energy reduction Δe (for $K = 1 \times 10^{-2}$ and $\tau = 0.25$ as in Figure 4).

The value of the ratio r defined by (42) depends strongly on the growth rate β. In the present formulation, β is determined by the nondimensional parameter K and by the rate of the friction velocity U_* to the propagation speed C for the most rapidly growing wave; see (38). To further examine the sensitivity of the ratio r, we apply values from previous studies of waves in a saturated sea: $\tau = 0.4$ [*Weber and Melsom*, 1993b] and $K = 2.7 \times 10^{-2}$ [*Mitsuyasu and Honda*, 1982]. The resulting functional dependence of r on ν is displayed in Figure 5a by curve 2. Note that this yields a somewhat larger contribution from the drift induced by wave breaking compared to curve 1. Also, keep in mind that the choice of parameters for curve 2 is inconsistent with (39) and (40).

When the energy that is lost from the periodic motion during breaking is small, the surface drift that is induced by a single breaking event becomes relatively small, too. However, a small loss of energy in each breaking event corresponds to a high frequency of such events (assuming that the growth rate β is not affected by this frequency). Thus the amount of energy that is lost in the breaking process does not influence the magnitude of the surface drift significantly. This is evident from Figure 5b, where the ratio r has been depicted as a function of the relative energy loss Δe.

In conclusion, it has been demonstrated in the present paper that the drift that is induced due to wave breaking is not much affected by either the parameterization of breaking events or by the reduction of the wave amplitude due to the breaking process. However, the surface drift is sensitive to the estimates for the growth rate β and the eddy viscosity ν.

Acknowledgments. This work was made possible by the Norwegian Science Council (Norges Forskningsråd) under contract 100674/410. I am grateful for the financial support that has been provided by this council. The paper was written during my stay at the Center for Ocean-Atmospheric Prediction Studies (COAPS) at Florida State University, USA. I thank the COAPS team for their support and encouragement.

References

Ekman, V. W., On the influence of Earth's rotation on ocean currents, *Ark. Mat. Astron. Fys.*, *2*, 1-53, 1905.

Hasselmann, K., Wave-driven inertial oscillations, *Geophys. Fluid Dyn.*, *1*, 463-502, 1970.

Jacobs, S. J., An asymptotic theory for turbulent flow over a progressive water wave, *J. Fluid Mech.*, *174*, 69-80, 1987.

Lamb, H., *Hydrodynamics*, 6th ed., 738 pp., Cambridge Univ. Press, New York, 1932.

Longuet-Higgins, M. S., Mass transport in water waves, *Philos. Trans. R. Soc. London A*, *245*, 535-581, 1953.

Longuet-Higgins, M. S., A nonlinear mechanism for the generation of sea waves, *Proc. R. Soc. London A*, *311*, 371-389, 1969.

Madsen, O. S., A realistic model for the wind-induced Ekman boundary layer, *J. Phys. Oceanogr.*, *7*, 248-255, 1977.

Melsom, A., Effects of variable eddy viscosity on wave-induced currents under ice, *Ann. Geophys.*, *11*, 78-88, 1993.

Melville, W. K., and R. J. Rapp, Momentum flux in breaking waves, *Nature*, *317*, 514-516, 1985.

Mitsuyasu, H., A note on the momentum transfer from wind to waves, *J. Geophys. Res.*, *90*, 3343-3345, 1985.

Mitsuyasu, H., and T. Honda, Wind induced growth of water waves, *J. Fluid Mech.*, *123*, 425-442, 1982.

Phillips, O. M., The equilibrium range in the spectrum of wind generated waves. *J. Fluid Mech.*, *4*, 426-434, 1958.

Phillips, O. M., *The Dynamics of the Upper Ocean*, 2nd ed., 336 pp., Cambridge Univ. Press, New York, 1977.

Plant, W. J., A relationship between wind stress and wave slope, *J. Geophys. Res.*, *87*, 1961-1967, 1982.

Stokes, G. G., On the theory of oscillatory waves, *Trans. Cambridge Philos. Soc.*, *8*, 441-455, 1847.

Toba, Y., Local balance in the air-sea processes, III, On the spectrum of wind waves, *J. Oceanogr. Soc. Jpn.*, *29*, 209-220, 1973.

Ursell, F., On the theoretical form of ocean swell on a rotating Earth, *Mon. Not. R. Astron. Soc. Geophys. Suppl.*, *6*, 1-8, 1950.

Weber, J. E., Attenuated wave-induced drift in a viscous rotating ocean, *J. Fluid Mech.*, *137*, 115-129, 1983.

Weber, J. E. and E. Førland, Effect of the air on the drift velocity of water waves, *J. Fluid Mech.*, *218*, 619-640, 1990.

Weber, J. E., and A. Melsom, Transient ocean currents induced by wind and growing waves, *J. Phys. Oceanogr.*, *23*, 193-206, 1993a.

Weber, J. E., and A. Melsom, Volume flux induced by wind and waves in a saturated sea, *J. Geophys. Res.*, *98*, 4739-4745, 1993b.

A. Melsom, Norwegian Meteorological Institute, P.O. Box 43, Blindern, N 0313 Oslo, Norway (e-mail: a.melsom@dnmi.no)

(Received May 8, 1995; revised January 24, 1996; accepted January 30, 1996.)